Trends in Developmental Biology
Vol. 7, 2013

Original Communication

Ultrastructural observations on the scarring process in the cauterized tail and the amputated limb of lizard

Lorenzo Alibardi*

Dipartimento di Biologia evoluzionistica eperimentale, via Selmi 3, University of Bologna, 40126, Bologna, Italy

ABSTRACT

The cicatrisation in lizard tissues after cauterization of the stump in amputated tails has been compared to the cicatrisation of the limb after amputation. The stump is covered by an initial loose connective tissue that contains fibrin exudates. A dense connective outgrowth is later formed from the stump. Collagen fibrils, granulocytes, and macrophages are more common in the connective of the outgrowths than in the normal regenerative blastema. Inflammatory cells remain in cauterized tissues for a longer period (over 20 days post-trauma) than in the normal blastema. Among fibrin exudate numerous fibrocytes with extensive rough endoplasmic reticulum rapidly synthesize a banded type of collagen fibrils that turn the connective tissue into a scar. The regenerating spinal cord, pigment cells, and muscles are trapped in this scar and regeneration is blocked. Also in the limb stump, numerous leucocytes and macrophages are present among amputated tissues in conjunction with a lasting inflammatory condition. It is concluded that the permanence of inflammation in tissues of the tail stump after cauterization and in the limb after amputation determines the failure of tissue regeneration. The process of cicatrisation in lizards represents a model to analyze inflammation and scarring in homeotherm vertebrates.

KEYWORDS: lizards, tail, limb, cauterization, regeneration, scarring, ultrastructure

*alibardi@biblio.cib.unibo.it

INTRODUCTION

Tail regeneration in lizards is a common process that follows the loss of the tail, while a limited or no regeneration follows after the loss of the limb [1-10]. The remarkable process of tail regeneration in lizards, sometimes restoring over 30% of the original body mass lost after tail amputation, represents a unique case of regeneration among amniotes. This process has probably evolved in conjunction with the autotomous mechanism to escape predators [10-13]. The specific evolutionary pressure that selected tail regeneration in lizards somehow has removed the cell mechanisms inhibiting tissue growth and organ morphogenesis. Lizards therefore represent a very interesting model to analyze the factors limiting tissue regeneration in amniotes.

It has been proposed that scarring in mammalian tissues has been selected during evolution in order to quickly wall-off the massive bleeding and microbe penetration after injuries compatible with survival [14]. Wounding and re-epithelization in lizard tail and limbs follows the process seen in mammals but studies on the inflammatory response after tail or limb amputation have rarely been done [4, 13, 15-18].

In the limb, a small scar or occasionally an elongated cone appendage is formed within a month from amputation [2-4, 15]. The block of limb regeneration depends on a number of factors, including the extensive damage to the tissues that, as in mammalian wounds, leads to chronic inflammation and scarring [14, 19, 20].

It is known that different manipulations can induce delay or even failure of tail regeneration in lizards. These include covering of the stump with old skin flaps, cauterization or wounding the regenerating blastema, or chemical treatments such as using Nitrogen mustard, Berillium or Cadmium nitrate [1, 5, 10, 13]. Although it is likely that most of these manipulations cause an increase in the inflammatory reaction of the damaged tissues, no fine structural description that sustains this hypothesis have been documented. It is also likely that the inflammatory reaction of the scarring tail resembles the natural process occurring in the limb but an ultrastructural comparison between the two processes is needed. The present electron microscope study describes the cellular response after tail cauterization (heat-damaged) and the inflammatory reaction present in the amputated limb, and compares the two processes to the cellular response present during normal tail regeneration.

MATERIALS AND METHODS

The present study has been conducted on adult lizards (*Podarcis sicula*) of both sexes. The animals were kept in a terrarium at 27-33°C and with a photoperiod of 12-14 hours of light. Lizards were kept and manipulated following institutional guidelines for animal care and handling.

The tail was amputated at about 1/3 proximal, by twisting the tail to induce autotomy. Five tails were left to regenerate normally. After the regenerating blastema was formed in normal (control) tails, at 12-15 days post-amputation it was removed and fixed in glutaraldehyde, as detailed below.

In sixteen autotomized, ether anesthetized lizards (10 *Podarcis sicula* and 6 *Tarentola mauritanica*), the tail surface was cauterized by passing a red-hot spatula for 10-15 seconds over the stump as to turn the surface brown. The spinal cord inside the vertebral canal was not specifically cauterized in this experiment. After 15 days from cauterization, the healed stump contained a blastema-like outgrowth that was collected (3 samples for *P. sicula*) for fixation in glutaraldehyde and embedding in Epon resin (see below). Two other samples of *P. sicula* were collected as short mounds of 2-3 mm with the beginning of scaling (3 weeks), and were fixed in 10% formaldehyde (see below). The other samples (the remaining 5 samples of *P. sicula* and all the 6 samples of *T. mauritanica*) were left to regenerate until 35 and 40 day post-cauterization (Table 1). After this period the tail outgrowths were fixed in 10% formaldehyde for one day, dehydrated and embedded in wax. After sectioning using a rotatory microtome, these sections were stained with hematoxylin-eosin for the histological study.

In thirteen ether-anesthetized lizards (*P. sicula*), the posterior limb was amputated above the knee, and the animals were left to heal up to 22-23 days post-amputation. The protruding femur on the stump surface was cut off to leave an even surface to heal. Tissue were collected at 3-4 days (3 samples), 6-7 days (2 samples), 12-13 days (2 samples), 17-18 days (4 samples) and 22-23 days (2 samples) days post-amputation, and fixed with glutaraldehyde for the ultrastructural study (see below).

Table 1. Examples of tail outgrowths resulted after cauterization of the tail stump (n = number of cases). Scars are scaled and stubby-shaped. Tails are shorter and thinner in comparison to normally regenerated tails.

Podarcis sicula (35 days post-amputation, n = 6)	*Tarentola mauritanica* (40 days post-amputation, n = 6)
Scar of 1 mm with trapped ependyma	Scar of 1 mm with trapped ependyma
Scar of 2 mm with trapped ependyma	Scar of 2 mm with trapped ependyma
Scar of 2 mm with trapped ependyma	Scar of 3 mm with trapped ependyma
Scar of 2 mm with trapped ependyma	Short tail of 4 mm with trapped ependyma
Scar of 3 mm with trapped ependyma	Thin tail of 11 mm with ependyma, cartilage but scarce muscles
Thin tail of 7 mm with ependyma, cartilage but scarce muscles	Thin tail of 12 mm with ependyma, cartilage but scarce muscles

Tissue to be embedded in plastic resin, were rapidly fixed at 0-4°C in 2.5% glutaraldehyde in 0.12 M Phosphate buffer at pH 7.2 for 8 hours. The fixed tissues were rinsed in the buffer, osmicated for 90 min (2% OsO_4), dehydrated in ethanol, then propylene oxide for 40 min, embedded in Epon Resin at room temperature for 12 hours, and cured for 2 days at 60°C.

Representative stages of normal regenerated blastemas of the tail, from healing cauterized tail, and in the healing limb, were mainly sectioned in longitudinal section and few cases in cross section under an ultramicrotome or rotatory microtome. Thick (1-2 μm for plastic sections, and 5-8 μm for wax sections) and thin (40-90 nm) sections were collected onto glass slides. Plastic thick sections were stained in 1% toluidine blue for the histological study. Thin sections were collected on copper grids and routinely stained with uranyl acetate and led citrate, rinsed, dried, and observed under an EM-300 Philips and Hitachi-600 transmission electron microscopes. Images were collected as photographical pictures, and were scanned and digitalized into a computer, and figure plates were composed using a Photoshop Program.

RESULTS

Cell composition of normal tail blastema

The normal regenerating blastema of the tail at 12-15 days post-amputation appeared as a round, dark and soft outgrowth over the tail stump (Fig. 1A). The histological examination of the blastema showed that it was made of a loose mesenchymal tissue beneath the wound epidermis (Fig. 1B). The mesenchyme also surrounded the tip of the regenerating spinal cord represented by the ependymal canal that formed a terminal ependymal ampulla. The larger part of the numerous melanocytes of the blastema were seen in the tissues surrounding the apical ependymal and concentrated mainly beneath the epidermis (melanophores) or within the basal layer of the epidermis. The resulting blastema was homogenously dark-pigmented.

The ultrastructural analysis of the blastema of normal regenerating tail showed mesenchymal cells mixed with prevalently elongated, fibroblast-like cells. The latter produced long and irregular elongation contacting broad intercellular spaces containing amorphous material of likely glycosaminoglycan composition and few collagen fibrils (Fig. 1C, D). The rough endoplasmic reticulum and the Golgi apparatus were little

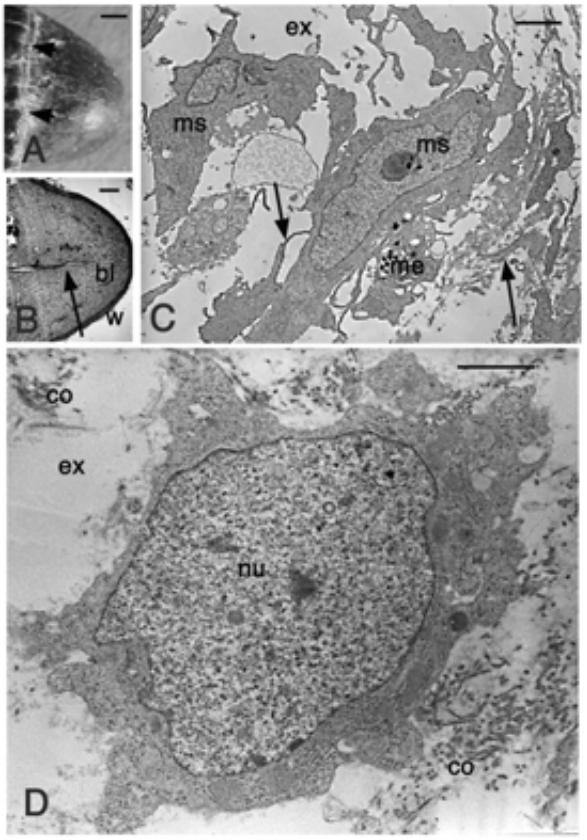

Fig. 1. Gross (**A**), histological (**B**) and ultrastructural (**C, D**) aspects of the normal blastema at 15 days post-autotomy in *P. sicula*. **A**, normal blastema (arrows point the connection to the tail stump). Bar, 0.5 mm. **B**, histological view of a blastema revealing the mesenchymal composition and the elongation of the regenerating spinal cord in the form of an ependymal tube (arrowhead). Arrows indicate differentiating muscles. Bar, 40 μm. **C**, mesenchymal cells have numerous cytoplasmic processes (arrows) and the large extracellular spaces contains little intercellular matrix or collagen fibrils. Bar, 2 μm. D, detail of mesenchymal cells with large, euchromatic nucleus, surrounded by electron-pale extracellular material (typical for glycosaminoglycans) and few, isolated collagen fibrils. Bar 1 μm. **Legends**: bl, blastema; co, collagen fibrils; ex, extracellular spaces; ms, mesenchyma cell; me, melanophore; nu, nucleus; w, wound epidermis.

developed in mesenchymal cells, while in more elongated fibroblasts some short cisternae of the rough endoplasmic reticulum were present (Figs. 1D, 2A).

Among mesenchymal cells and fibroblasts, some macrophages were also present (Fig. 2B, C). These cells showed variably long filopodia contacting the scarce amorphous matrix of the blastema or also the surface of mesenchymal cells. The Golgi apparatus of macrophages was surrounded with numerous small vesicles and electron-dense lysosomes. Large (0.5-1.0 μm) secondary lysosomes containing material in course of digestion were occasionally seen in these cells. The nucleus presented a variable degree of heterochromatine clumps. Other cell types in the blastema were sparse blood cells within blood capillaries (see further details in 9).

Cell composition after tail cauterization

Following the lesion, the tissues on the stump surface of the tail formed a dark, burnt surface made of necrotic tissues (data not shown).

After 2-5 days on the surface of the stump, a dark and thick scab was formed which in some cases fell down at 14-16 days post-cauterization revealing a soft, dark or pale shiny surface. In other cases, a mound of less than 1 mm in length resembling a regenerating blastema appeared after the loss of the scab (data not shown). The soft mound formed over the healed stump became pale and started to form scales within the following 4-6 days, so that at 20-22 days post-cauterization a pale, scarring mound with little scaling was present. This scarring outgrowth formed irregularly distributed scales at 30-40 days post-cauterization (Fig. 3A).

The histological analysis of outgrowths at 15-17 days post-cauterization showed beneath the multilayered epidermis, the accumulation of fibroblasts that formed a dense connective in comparison to the soft, mesenchymal connective present in a normal blastema (Fig. 3B-D). The ultrastructural analysis of the small, still soft outgrowths at 14 days post-cauterization showed some variations from the structure observed in the normal blastema. The tissue was made of typical fibroblasts containing a developed ergastoplasmic reticulum, surrounded by a fibrinous exudate containing banded collagen fibrils (Fig. 3C, D).

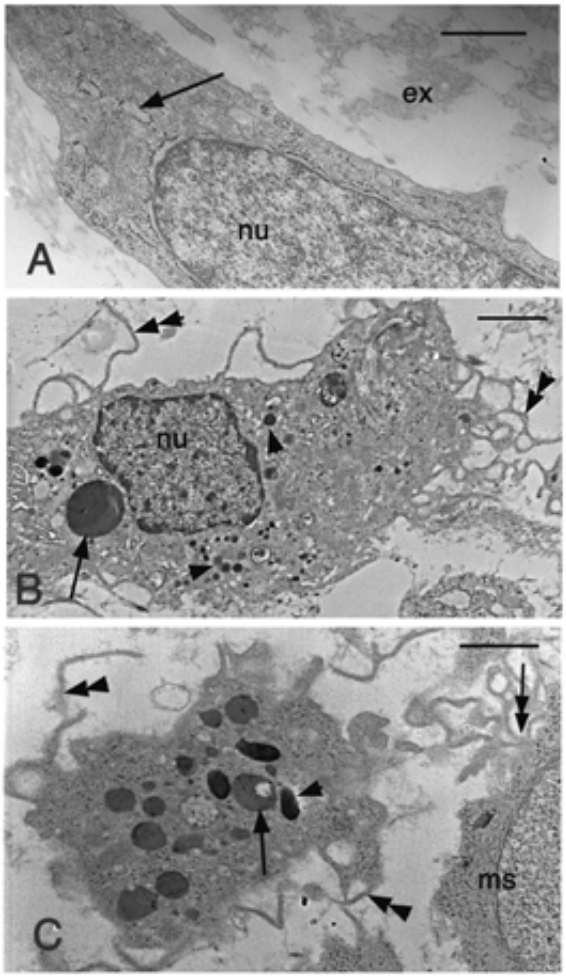

Fig. 2. Ultrastructural details of more common cells found in the normal blastema at 15 days post-autotomy in *P. sicula*. **A**, detail of an elongated mesenchymal cell containing short ecisternae or endoplasmic reticulum (arrow). Only amorphous material (glycosaminoglicans) is seen in the extracellular matrix. Bar, 1 μm. **B**, general view of macrophage with small primary lysosomes (arrowheads) and few large digestive vacuoles (arrow). Double arrowheads indicate extensive folded filopodia. Bar, 2 μm. **C**, detail of part of a macrophage showing that filopodia contact (double arrow) a mesenchymal cell through filopodia (double arrowheads). The arrow points to a secondary lysosome and the arrowhead to a denser primary lysosome). Bar, 1 μm. **Legends**: ex, extracellular space with matrix material; ms, mesenchymal cell; nu, nucleus.

The cytoplasm of some fibroblasts also revealed the presence of sparce bundles of microfilaments that indicated these cells might represent actin-containing myofibroblasts (Fig. 3D inset).

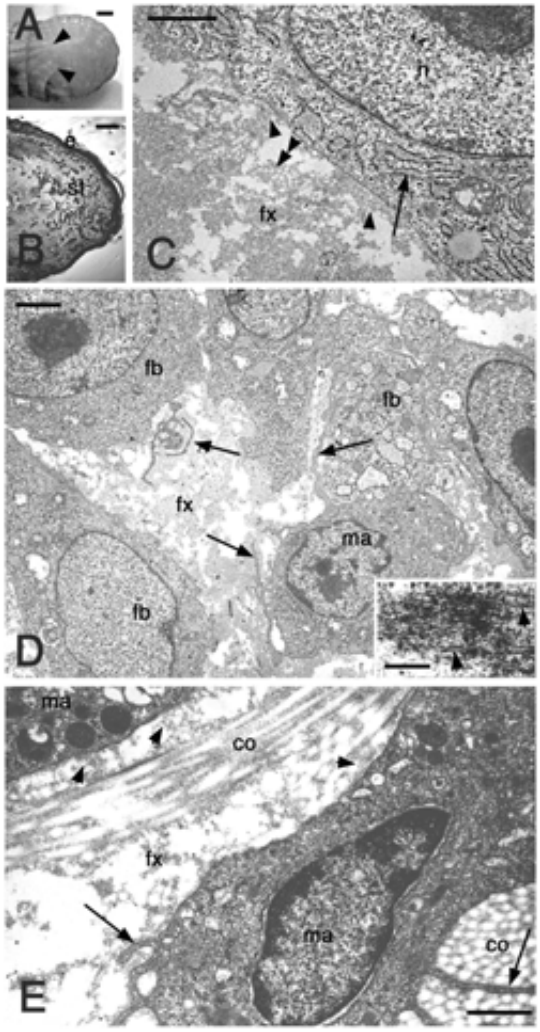

Fig. 3. Gross (**A**), microscopic (**B**) and ultrastructural (**C**-**E**) aspects of mounds derived from tail stump cauterization (15 days in **C**-**E**) in *P. sicula*. **A**, pale and scaled (arrowheads) cicatrix at 35 days post-cauterization. Bar, 0.5 mm. **B**, longitudinal section at 22 days post-cauterization of an outgrowth containing numerous pigment cells. Bar, 50 μm. **C**, detail showing the electron-pale meshwork pattern of the matrix material (double arrowhead) contacting (arrowheads) a fibroblast with developed ergastoplasmic reticulum (arrow). Bar, 0.5 μm. **D**, groups of fibroblasts connected to macrophages (arrows on filopodia) through the fibrinous exudates. Bar, 1 μm. The inset shows a small bundle of filaments (arrowheads) of unknown composition sometimes seen in these fibroblasts. Bar, 200 nm. **E**, macrophage apparently trapped (arrows indicate the filopodia) within the electron-pale meshwork pattern, collagen meshwork. Fibrinous exudates also contact macrophages (arrowheads). Bar, 1 μm. **Legends**: co, collagen fibrils (electron-pale); e, epidermis; fb, fibroblast; fx, fibrin exudates; ma, macrophage; n, nucleus; st, scar tissue.

Numerous macrophages were also present which contacted both the dense fibrinous material and the fibroblasts (Fig. 3D). In scattered regions of the tissue, collagen fibrils were more numerous and organized in bundles of fibrils, producing a characteristics electron-pale meshwork pattern in the extracellular matrix. Both fibroblasts and macrophages in these patched areas appeared as trapped within the collagenous material (Fig. 3E). Another common cell types encountered among fibroblasts were electron-dense granulocytes with large, 0.2-0.5 μm granules (Fig. 4A). The study at high magnification of the granules showed a characteristics spongy texture (Fig. 4A inset). The cell surface contained short cytoplasmic blebs, indicating that these cells were tentatively moving among the dense extracellular matrix. Another frequent cell type was melanophores, and these cells also appeared trapped within the dense extracellular matrix of the stump (Fig. 4B).

Collagen fibrils were numerous not only among the fibrinous matrix of the inner mass of fibroblasts but also beneath the epithelium of the outgrowths. In these region a continuous dense lamella was present between dermis and epidermis, and the lamella was contacted by frequent anchoring fibrils (Fig. 4C). Hemidesmosomes were frequently seen along the basement membrane, like in the normal, fully differentiated epidermis. At 16-20 days after cauterization the connective of the outgrowth was made of elongated fibrocytes among which a dense matrix containing numerous banded collagen fibrils was present.

The long-term effects of the cauterization on regeneration were seen examining samples after 35-40 days (Table 1 and Fig. 5). Only in few cases regenerated tails over 1 cm in length were obtained, but these appeared thinner and shorter than normal regenerated tails. Few muscle bundles were present inside these scaled tails. The distribution of pigment cells was more irregular than in regenerating blastema, and only few melanocytes were localized beneath the epidermis. Instead, a large number of pigment cells remained irregularly distributed within the connective tissues of the mound or in the growing outgrowths.

The histological examination of the short regenerated tails and of the cicatrix obtained after

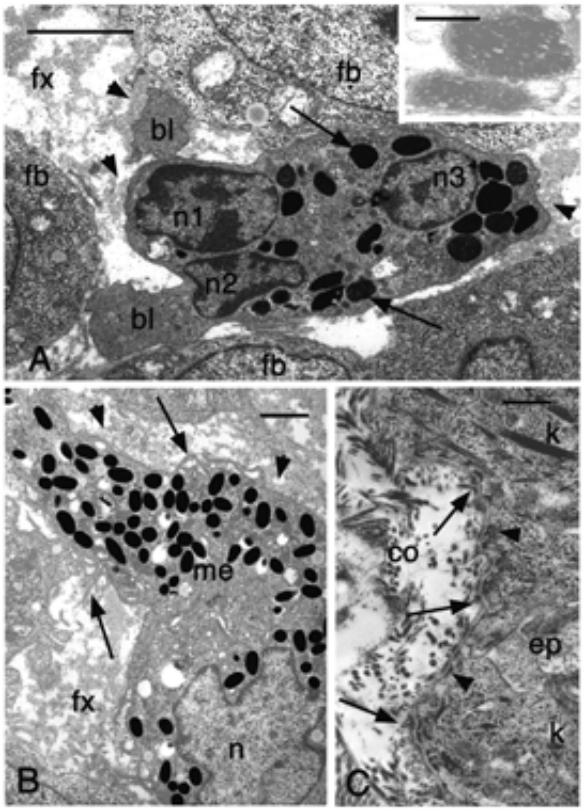

Fig. 4. Ultrastructure of cells of a mound at 15 days post-cauterization in *P. sicula*. **A**, detail of a granulocyte with blebs between fiblobasts and surrounded by fibrinous exudates (arrowheads). Arrows indicate azurophilic granules and a detail of their spongy-texture is shown in the inset at higher magnification (Bar, 250 nm). Bar, 2 μm. **B,** dermal melanophore (arrows on filopodia) surrounded by a fibrin exudates (arrowheads). Bar, 1 μm. **C**, detail of the basement membrane of basal keratinocyte with hemidesmosomes (arrowheads) and numerous collagen fibrils contacting the lamella densa (arrows). Bar, 0.5 μm. **Legends**: bl, cytoplasmic blebs of the granulocyte; co, collagen fibrils; ep, epidermal cell; fb, fibroblast; fx, fibrinosus exudates in the extracellular space; k, keratin bundles; me, melanophore; n, nucleus (n1, n2, n3, lobated parts of granulocyte nucleus).

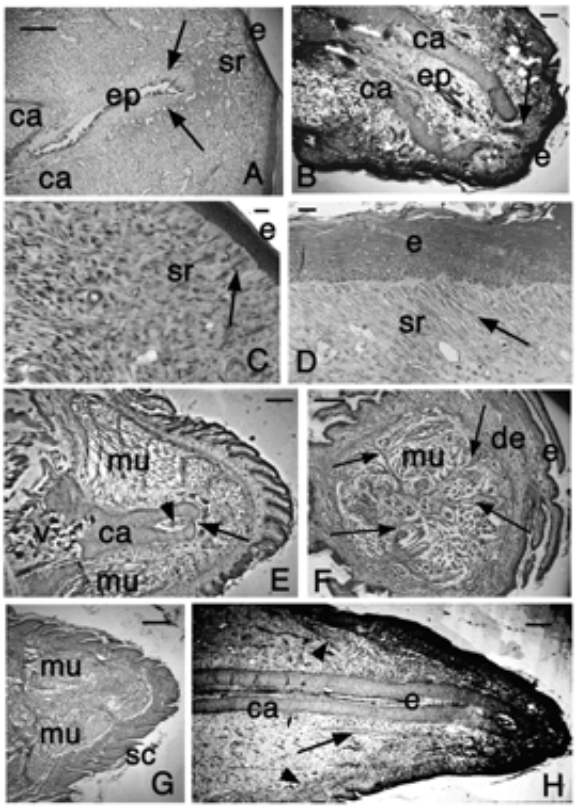

Fig. 5. Histological aspects of cicatrix tails (**A-D**) and of a regrown tail (**H**) at 35 days post-cauteriztion in *P. sicula* and after 40 days in *T. mauritanica* (**E-G**). Haematohylin-eosin stain in all sections. **A**, regenerating ependymal tube trapped by the scarring connective (arrows). Bar, 100 μm. **B**, short regenerate with cartilaginous tube surrounding the ependyma which is trapped by apical scar tissue (arrow). Bar, 100 μm. **C**, detail of scar tissue in lateral area of a tail cicatrix of 3 weeks. Note fusiform fibrocytes (arrow) contacting the epidermis. Bar, 10 μm. **D**, apex of a tail scar at three weeks of regeneration. Beneath the thick wound epidermis numerous fusiform fibrocytes are seen (arrow). Bar, 10 μm. **E**, short tail with heavy scalation and short cartilaginous tube that traps (arrow) the ependyma (arrowhead). Bar, 200 μm. **F**, cross section of short tail (3 mm long) were mainly muscle bundles subdivided by connective septa (arrows) and dense connective are present. Bar, 200 μm. **G**, short tail like in the previous figure but shown in longitudinal section. Muscle bundles occupy most of the volume of this outgrowth. Bar, 200 μm. **H**, long regenerated tail with cartilaginous tube and ependyma but scarce muscle bundles (arrowheads). The arrow indicates a big ventral nerve. Bar, 200 μm. **Legends**: ca, regenerated cartilaginous tube; de, dense dermis; e, epidermis; ep, ependyma; mu, muscle bundles; sc, scales; sr, scarring connective tissue.

cauterization showed that the regenerating ependymal tube appeared trapped by the surrounding dense connective (Fig. 5A, B). Beneath the epidermis, fibrocytes often showed a perpendicular orientation with respect to the basement membrane (Fig. 5C, D). In short tails of 2-3 mm, the ependyma appeared to have initially regenerated inside a short cartilaginous tube but was later trapped within a scar connective

or fibrocartilage (Fig. 5B, E). In other 2-4 mm long tails, only muscles were regenerated but neither ependyma nor cartilaginous tissue were present (Fig. 5F, G). In the longer regenerated tails indicated in Table 1, a cartilaginous tube containing the ependyma was formed but few muscle bundles were regenerated, surrounded by adipose and connective tissues (Fig. 5H).

Wound healing of the limb stump

The gross aspect of the healing stump of amputated limbs somehow resembled that of the scarring tail stumps after cauterization. A mound of soft tissue was initially formed after 14-18 days post-amputation, and in the following days it turned pale and consistently hard. Eventually the mound at 25-35 days post-amputation formed a 0.5-2.0 mm long outgrowth scar, occasionally with protruding short appendages (Fig. 6A). The histological analysis of the longer limb outgrowths at 17-18 days post-amputation showed the presence of a loose connective made of fusiform fibroblasts beneath the stratified epidermis (Fig. 6B). At 22-23 days post-amputation this connective tissue contained numerous fibrocytes and a dense extracellular matrix, forming a scar connective.

The ultrastructural aspect of healing tissues at 3-4 and 6-7 days post-amputation of the limb showed an intense inflammatory reaction, somehow similar to that of a cauterized tail. Numerous granulocytes and some macrophages were present beneath the scab at these stages, and were involved mainly in phagocytosis of bacteria and degenerating cells after wounding (Fig. 6C). Granulocytes showed an electron-dense nucleus with heterochromatine, and contained digestive vacuoles and a variable number of activated azurophyl granules with a spongy texture (inset in Fig. 6D). Macrophages contained few granules and large digestive vacuoles, a pale nucleus with heterochromatine and sparse filopodia on their cell surface.

At 12 days post-injection macrophages among fibrobalst were more numerous than in early stages, although also numerous granulocytes were still present (Fig. 6D). Mesenchymal cells, as those present in the blastema of a normal regenerating tail, were uncommon over the limb stump in which, mainly fibrobasts surrounded by collagen fibrils were seen.

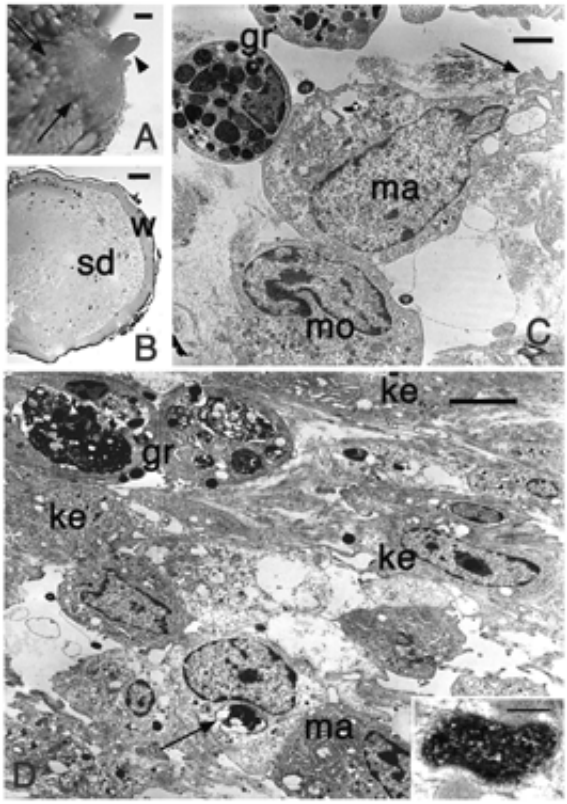

Fig. 6. Gross (**A**), microscopic (**B**) and ultrastructural aspects (**C, D**) of hind limb regeneration. **A**, after 25 days from the level of amputation (indicated by arrows) a scar has formed with a thin outgrowth (arrowhead). Bar, 0.3 mm. **B**, longitudinal section of mound at 18 days post-amputation. Beneath a thick wound epithelium a mass of fibroblasts is present. Bar, 80 μm. **C**, free granulocytes and macrophages (the arrow points to a phagosome) present among keratinocytes of the wound epidermis at 12 days post-amputation. Bar, 2.5 μm. **D**, Bar, 1 μm. **Legends**: gr, granulocyte; ke, keratinocyte; ma, macrophage; mo, monocyte; sd, scarring dermis; w, wound epidermis.

Macrophages were the prevalent phagocytes present at 16-22 days post-amputation while numerous fibroblasts producing collagen fibrils were present in the mound (Fig. 7A). These connective cells showed a developed endoplasmic reticulum and Golgi apparatus with dilated cisternae accumulating pro-collagen molecules. The cells were surrounded by numerous non-banded and banded collagen fibrils. In random areas of the inner mass of scarring connective, some large bundles of collagen were formed, especially beneath the epidermis (Fig. 7B). Numerous collagen fibrils contacted the basement

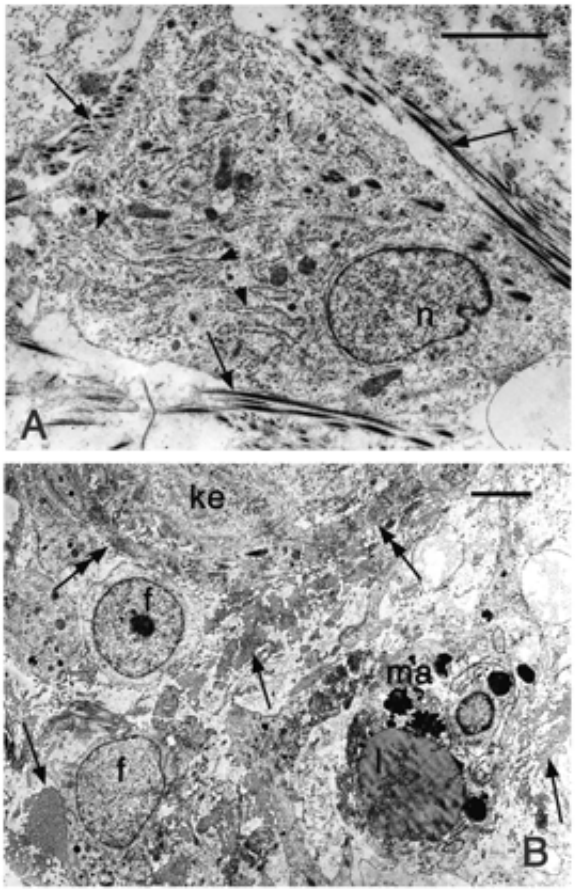

Fig. 7. Ultrastructural aspects of limb stump at 18 days post-amputation. **A**, detail of fibroblast actively producing collagen as indicated by the well developed endoplasmic reticulum (arrowheads) and from the numerous extracellular collagen fibrils (arrows). Bar, 2.5 μm. **B**, detail of superficial dermis where numerous collagen bundles are present (arrows) among fibroblasts, including those beneath the epidermis (double arrows). A phagocyte has formed as large lipid droplet (arrowhead). Bar, 2.5 μm. **Legends**: f, fibroblast; ke, keratinocyte (epidermis); l, lipid droplet; ma, macrophage; n, nucleus.

membrane of this epithelium where a lamella densa was well evident (data not shown).

At 22 days post-amputation, among the dense, mainly collagenous extracellular matrix, sparse macrophages were still seen, while occasionally granulocytes were also seen.

DISCUSSION

The present study has shown that the block of tissue regeneration in the lizard tail is the induction of a strong inflammatory response with consequent scarring, like in the lizard limb and in mammalian wounds [14, 21]. The common feature observed in scarring outgrowths formed on lizard tails is the change of the color from pink or dark into a paler and scaling mould. After 20-25 days from the injury, this outgrowth rapidly looses the soft texture and becomes hard and heavily scaled. This reflects the change from the initial soft and vascularized connective that is rapidly replaced by an irregular, collagen-rich connective. Trapping of melanophores among the dense fibroblast network within the tissues of the outgrowth may also contribute to the change of color in scars, since pigment cells remain inside the dense connective tissue that masks their pigmentation.

The rapid formation of a differentiated basal lamina with a continuous dense lamella in both cauterized tail stump and in the amputated limb contrasts with the presence of a discontinuous lamella densa in the blastema of the regenerating tail [17, 22]. The strong inflammatory reaction that occurs in the amputated limb can also be induced in the tail stump through cauterization or other experimental manipulation [1, 10]. The cauterization, aside tissue necrosis, also produces damage in the permeability of blood vessels with the consequent loss of large amount of fibrin. The latter is still present among tissues at 15 days post-cauterization. The extravasation of fibrin is a common process occurring during early stages of mammalian wounds [23-25], but it appears a more relevant and lasting process in reptilian tissues connected to their resistance to infections [26].

The damage of the perivascular connective induced by the heat damage may stimulate the formation of reactive cells, by local proliferation or migration from the blood. In mammalian connectives, migrating cells during inflammation give rise to a population of myofibroblasts [19, 27]. These migrating fibrocytes may even derive from the epidermis through a process of epidermal-dermal transformation [20]. The numerous macrophages and heterophyl granulocytes present for over 20 days post-injury in cauterized tissues of the tail and in the stump of the limb, probably stimulates the recruitment of scarring fibroblasts, a phenomenon well known for mammalian chronic inflammation and scarring. Despite the

ultrastructural features have indicated the presence of microfilaments and sparse bundles in scarring fibroblasts of lizards, it is unknown whether these cells also contain «alpha-smooth muscle actin microfilaments», the marker for scarring myofibroblasts in mammalian cells [20]. Myofibroblasts have been implicated in the rapid contraction of the wound and in the deposition of collagen.

In scars, not only the cell composition is changed in comparison to normal blastema but also the rate of degradation of the collagen by matrix proteases might be affected. It is known that in mammalian wounds, when components of the extracellular matrix, especially collagen, are degraded at lower rate than the production the net increase of collagen produces scarring [20]. Although there are no data on matrix proteases in lizard blastema, it is known that acid phosphatase, a lysosomal enzyme, increases in regenerating blastema and in more distal tissues of the regenerating tail in comparison to normal or more proximal tissues of the regenerating tail [28]. This suggests that degradation of intercellular matrix, together with the production of glycosaminoglycans such as jaluronate, favor cell migration. The latter is needed for covering the stump with new cells, for the distal growth and re-organization of the segmental muscles, and for the growth of the new spinal cord [8].

These observations indicate that the lizard model of regeneration can be utilized to study scarring mechanisms in amniotes in general, as it resembles the process in mammals [21, 27]. The condition of the mesenchyme and extracellular matrix in the normal regenerative tail blastema are comparable to those present in mammalian embryos or fetuses. It is known that mammalian fetal wounds produce little or no inflammation and that they repair with no scarring [14, 29, 30]. When cauterization or other strong injuries are made in fetal tissues, macrophages infiltrate in the damaged area and scarring is derived [30]. Among other cytokines, transforming growth factor Beta 1 (TGF-β1), produced by macrophages, stimulate fibrocyte recruitment [14]. Unlike in the adult condition, in embryonic and fetal wounds an isoform of TGF indicated as TGF-β3 is increased and this growth factor appears to promote regeneration without scarring. Further studies on the lizard model of tissue regeneration will test the presence of TGFs in normal tissues of the regenerating tail versus the tissues of a cauterized tail and from scarring tissues of the limb, to check whether reptiles also utilize these cytokines for tissue regeneration.

ACKNOWLEDGMENTS

The study was mainly conducted by personal funding, and under an Italian MPE 60% Grant in 2007.

REFERENCES

1. Marcucci, E. 1914-1915, Boll. Soc. Natur. (Napoli), 27-28, 249.
2. Marcucci, E. 1925, Boll. Soc. Natur. (Napoli), 38, 8.
3. Marcucci, E. 1930, Arch. Zool. Ital., 14, 27.
4. Barber, L.W. 1944, Anat. Rec., 89, 441.
5. Hughes, A. and New, D. 1959, J. Emb. Exp. Morph., 7, 281.
6. Simpson, S. 1965, Regeneration of the lizard tail. In: Regeneration in Animals and Related Problems. V. Kiortsis and H. A. L. Trampusch, (Editors): North-Holland, Amsterdam, 431-443.
7. Simpson, S. 1970, Amer. Zool., 10, 157.
8. Alibardi, L. and Sala, M. 1983, Atti Mem. Acc. Patav. Sci. Lett., Arti 95, 100.
9. Alibardi, L. and Sala, M. 1988, Boll. Zool., 55, 307.
10. Bellairs, A. d'A. and Bryant, S. V. 1968, Anat. Rec., 161, 489.
11. Arnold, E. N. 1984, J. Nat. Hist., 18, 127.
12. Reichman, O. J. 1984, Amer. Natur., 123, 752.
13. Alibardi, L. 2010b. Anat. Embryol. Cell Biol., 207, 1.
14. Ferguson, M. W. and O'Kane, S. 2004, Phil. Trans. Royal Soc., London, Series B, 359, 839.
15. Kudokotsev, V. P. 1960, Dok. Akad. Sci. SSSR, 126, 464-467.
16. Zika, J. M. 1969, J. Exp. Zool., 172, 1.
17. Alibardi, L. and Toni, M. 2005. J. Exp. Zool., 303A, 845.
18. Alibardi, L. 2010, Acta Zool., 91, 306.

19. Kovacs, E. J. and DiPietro, L. A. 1994, FASEB J., 8, 854.
20. Wynn, T. A. 2008, J. Pathol., 214, 199.
21. Kischer, C. W. 1984, Scan. Elect. Micr., 1984/I, 423.
22. Alibardi, L. 1994, Histol. Histopath., 9, 733-745.
23. Ross, R. and Odland, G. 1968a, J. Cell Biol., 39, 135.
24. Ross, R. and Odland, G. 1968b, J. Cell Biol., 39, 152.
25. Martin, P. 1997, Science, 276, 75.
26. Huchzermeyer, F. W. and Cooper, J. E. 2000, Vet. Rec., 147, 515.
27. DeLustro, F., Mackel, A. M., DeLustro, B. and LeRoy, E. C. 1983, Amer. Zool., 23, 213.
28. Alibardi, L. 1998. J. Zool., 246, 379.
29. Adzick, N. S. and Longaker, L. M. 1992, Fetal wound healing, Elsevier, New York.
30. Nodder, S. and Martin, P. 1997, Anat. Embryol., 195, 215.